AVF inversion of reflections from an anelastic target

K. A. Innanen, Dept. of Geoscience, Univ. Calgary, CREWES

SUMMARY

Certain seismic data anomalies, associated with low-Q targets, have recently been identified as instances of "absorptive reflectivity". The anelastic reflection coefficients underlying this type of anomaly, and their variations with frequency (AVF) and/or angle (AVA), represent a potentially important source of information for determining subsurface properties of relevance to reservoir characterization. Series expansions of absorptive reflection coefficients about small parameter contrasts and incidence angles can be used to separately estimate variations in anelastic target parameters through a range of direct formulas, both linear and with nonlinear corrections. Algorithmically, it is a differencing of the reflection coefficient across frequencies that separates Q variations from variations in other parameters. This holds for both two-parameter (P-wave velocity and Q) problems and five-parameter anelastic problems, and would appear to be a general feature of direct absorptive inversion.

INTRODUCTION

The geophysics literature contains numerous reports of frequency dependent seismic data anomalies associated with attenuating targets. Some researchers have attributed these to the presence of a strong absorptive reflection coefficient, which, indeed, according to wave theory places a characteristic imprint on the data. This represents a potentially important source of information of direct relevance in reservoir characterization, because, as we will demonstrate, variations in the reflection coefficient associated with a plane contrast in anelastic or an-acoustic medium parameters (discussed in theory by, e.g., White, 1965; Borcherdt, 1977; Kjartansson, 1979; Krebes, 1984; Lam et al., 2004; de Hoop et al., 2005; Borcherdt, 2009) contain in principle sufficient information to separately determine relative changes in these parameters at the point of contrast. That this is true is in fact a prediction of absorptive inverse scattering theory, which, in the limit as a set of absorptive volume scatterers combine to produce a specular reflector, has been shown to make use of these absorptive reflection amplitudes (Innanen and Weglein, 2007; Innanen and Lira, 2010). In this paper we derive a range of formulas designed to exploit this information, providing direct estimates of target absorptive medium properties, both in linearized forms and with non-linear corrections, given the reflection coefficient (which must be first derived from seismic data) as input.

An absorptive reflection coefficient can be analyzed mathematically by considering either its frequency variations (i.e., AVF), or its angle variations (i.e., AVA). Both have been studied: numerically, absorption-specific reflection coefficient variability has been reported at large angles when synthetic viscoelastic data were examined at fixed frequencies (Samec and Blangy, 1992). And more recently, field data variability associated with low-Q, fluid filled reservoirs has been attributed to "strongly frequency dependent" reflection coefficients (Odebeatu et al., 2006). This latter observation appears to be supported by other recent investigations and discussions (Chapman et al., 2006; Lines et al., 2008; Ren et al., 2009; Quintal et al., 2009). In this paper we will focus on AVF variations.

The estimation approach we take is straightforward: we express the reflection coefficient in terms of plane-wave variables incidence angle and frequency, expand it about small parameter contrasts and incidence angles, and directly invert these series to determine the properties of the target. We treat two cases: the reflection coefficient associated with, first, a two-parameter acoustic/absorptive contrast, and, second, a five-parameter anelastic contrast. The inversion is, in essence, a simplified form of inverse scattering. It represents a modification of a framework that has led elsewhere to direct acoustic and elastic target identification (Zhang and Weglein, 2009a,b). In addition to the added complication of absorbing media, in our approach rather than posing the full inverse scattering problem, thereafter reducing to the case of a single interface, we begin with a representation of the wave response of a single interface, i.e., the reflection coefficient. The cost is a loss of generality and applicability to problems outside of the framework of interest in this paper, but we benefit in that the formulas are derived rapidly.

ABSORPTIVE REFLECTION COEFFICIENTS

We consider a plane compressive (P-) wave, in a non-attenuating medium of incidence, impinging at an oblique angle θ on a boundary below which is an attenuative target medium. In a two-parameter absorptive/acoustic framework, the associated reflection coefficient is

$$R(\omega,\theta)=\frac{c\cos\theta-c_0\left[1+\frac{F}{Q}\right]\sqrt{1-\frac{c^2}{c_0^2}\left[1+\frac{F}{Q}\right]^{-2}\sin^2\theta}}{c\cos\theta+c_0\left[1+\frac{F}{Q}\right]\sqrt{1-\frac{c^2}{c_0^2}\left[1+\frac{F}{Q}\right]^{-2}\sin^2\theta}}, \quad (1)$$

where c_0 is the wavespeed in the incidence medium, c and Q are the wavespeed and quality factor of the target medium respectively, and $F=F(\omega)=i/2-1/\pi\log(\omega/\omega_r)$, ω_r being a reference frequency which we will assume is known. In Figure 1 the frequency dependence at normal incidence of R in the nearly constant Q case is illustrated.

In an anelastic framework we may also form a reasonably simple expression for the associated P and S wave reflection coefficients, beginning with the Zoeppritz equations for an incident elastic P-wave, which may be solved for instance by using Cramer's rule (Keys, 1989). We modify them to correspond to an incidence medium with P-wave velocity α_0, S-wave velocity β_0, and density ρ_0, and a target medium in which we introduce a compressional quality factor Q_P and a shear quality factor Q_S in addition to target α, β, ρ values. Using the definitions $X=\sin\theta$, $S_Y=\sqrt{1-Y^2X^2}$ and $S^Y=(1-2Y^2X^2)$ where Y can take on the values 1, B, C or D, we have

$$\mathscr{A}\begin{bmatrix}R_P\\R_S\\T_P\\T_S\end{bmatrix}=\mathbf{b}, \quad (2)$$

where

$$\mathscr{A}=\begin{bmatrix}-X & -S_B & CX & -S_D\\ S_1 & -BX & S_C & DX\\ 2B^2XS_1 & BS^B & 2AD^2XS_C & -ADS^D\\ -S^B & 2B^2XS_B & ACS^D & 2AD^2XS_D\end{bmatrix}, \quad (3)$$

and $\mathbf{b}=(X,S_1,2BS_1X,S^B)^T$, and the constants A, B, C and D contain anelastic medium parameters:

$$\begin{aligned}&A=\frac{\rho}{\rho_0},\ B=\frac{\beta_0}{\alpha_0},\\ &C=\frac{\alpha}{\alpha_0}\left[1+\frac{F_P}{Q_P}\right]^{-1},\ D=B\frac{\beta}{\beta_0}\left[1+\frac{F_S}{Q_S}\right]^{-1},\end{aligned} \quad (4)$$

where

$$F_P(\omega)=\frac{i}{2}-\frac{1}{\pi}\log\left(\frac{\omega}{\omega_{r_P}}\right),\quad F_S(\omega)=\frac{i}{2}-\frac{1}{\pi}\log\left(\frac{\omega}{\omega_{r_S}}\right), \quad (5)$$

and as before ω_{r_P} and ω_{r_S} are reference frequencies, assumed known. Equation (2) may be solved for the P- and S-wave reflection coefficients R_P and R_S respectively. With this ultimate aim in mind, we also form the auxiliary matrix $\mathscr{A}_P$ by replacing the first column of $\mathscr{A}$ with **b**, and the auxiliary matrix $\mathscr{A}_S$ by replacing the second column of $\mathscr{A}$ with **b**. Further, looking ahead to the inversion component of this study, for angles less than 90° we may expand the elements of $\mathscr{A}$ containing instances of S_Y in series about $X = 0$. In this paper for simplicity we will make use of the small angle approximation $S_Y \approx 1 - (1/2)Y^2X^2$, but accuracy to any desired order can easily be maintained.

SERIES EXPANSIONS OF R, R_P AND R_S

We now express the reflection coefficients of the previous section as series in orders of both X and the perturbations that the incidence medium parameters experience in becoming the target medium parameters. Treating the acoustic/absorptive problem first, we define $a_c = 1 - c_0^2/c^2$ and $a_Q = 1/Q$, and expand equation (1) about these and small X, obtaining

$$\begin{aligned} &R(\omega,\theta) \\ &= \left[\left(\frac{1}{4}a_c - \frac{1}{2}Fa_Q\right) + \left(\frac{1}{8}a_c^2 + \frac{1}{4}F^2a_Q^2\right) + ...\right]X^0 \\ &+ \left[\left(\frac{1}{4}a_c - \frac{1}{2}Fa_Q\right) + \left(\frac{1}{4}a_c^2 - \frac{1}{2}Fa_ca_Q + \frac{3}{4}F^2a_Q^2\right) + ...\right]X^2 \\ &+ \left[\left(\frac{1}{4}a_c - \frac{1}{2}Fa_Q\right) + \left(\frac{3}{8}a_c^2 - Fa_ca_Q + \frac{5}{4}F^2a_Q^2\right) + ...\right]X^4 \\ &+ ... \quad . \end{aligned} \tag{6}$$

In Figure 2 the accuracies of first and second order truncations of R in equation (6) are illustrated; as one would expect, at large parameter perturbations and large angles, the approximation error of the first order approximation grows. This is technically true of the second order approximation, but the error is greatly reduced and does not grow significantly until comparatively large angles are considered. Second-order effects noticeably influence R for targets with $Q < 50$, which is the range of interest for us, hence we must anticipate nonlinearity to be an important issue in the inverse problem. In the anelastic case we define $a_\alpha = 1 - \alpha_0^2/\alpha^2$, $a_\beta = 1 - \beta_0^2/\beta^2$, $a_\rho = 1 - \rho_0/\rho$, $a_{Q_P} = 1/Q_P$, $a_{Q_S} = 1/Q_S$, substitute these forms into A, C, and D in equation (4), and expand the three results in series. When these are in turn substituted into $\mathscr{A}$, $\mathscr{A}_P$, and $\mathscr{A}_S$, with all S_Y quantities also expressed in series form, their determinants may be organized in increasing order in the five perturbations:

$$\begin{aligned} \det\mathscr{A} &= \det\mathscr{A}^{(0)} + \det\mathscr{A}^{(1)} + \det\mathscr{A}^{(2)} + ..., \\ \det\mathscr{A}_P &= \det\mathscr{A}_P^{(1)} + \det\mathscr{A}_P^{(2)} + ..., \\ \det\mathscr{A}_S &= \det\mathscr{A}_S^{(1)} + \det\mathscr{A}_S^{(2)} + ..., \end{aligned} \tag{7}$$

where superscript (i) indicates i'th order in any combination of the five perturbations (e.g., a term containing $a_\rho^2 a_\beta$ is considered "third order"). Finally we generate series expressions for R_P and R_S in terms of the determinants in equation (7), also organized in increasing powers of the perturbations, using Cramer's rule:

$$R_P = \frac{\hat{\det}\mathscr{A}_P}{\hat{\det}\mathscr{A}} = \hat{\det}\mathscr{A}_P^{(1)} + \left(\hat{\det}\mathscr{A}_P^{(2)} - \hat{\det}\mathscr{A}_P^{(1)}\hat{\det}\mathscr{A}^{(1)}\right) + ..., \tag{8}$$

and likewise

$$R_S = \hat{\det}\mathscr{A}_P^{(1)} + \left(\hat{\det}\mathscr{A}_P^{(2)} - \hat{\det}\mathscr{A}_P^{(1)}\hat{\det}\mathscr{A}^{(1)}\right) + ..., \tag{9}$$

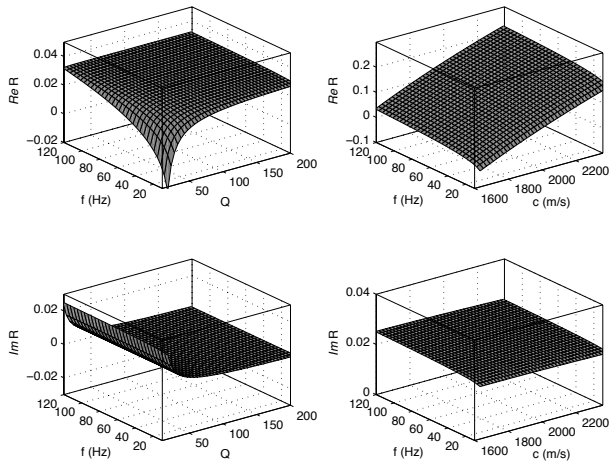

Figure 1: Absorptive reflection coefficient R at normal incidence, as expressed in equation (1) with $\theta = 0$, with c_0 =1500m/s. Left column: R for a range of frequency and Q values (c fixed at 1600m/s). Right column: R for a range of frequency and c values (Q fixed at 10). Each fixed Q value produces, in the real part of R, a unique associated signature in the frequency domain (top left).

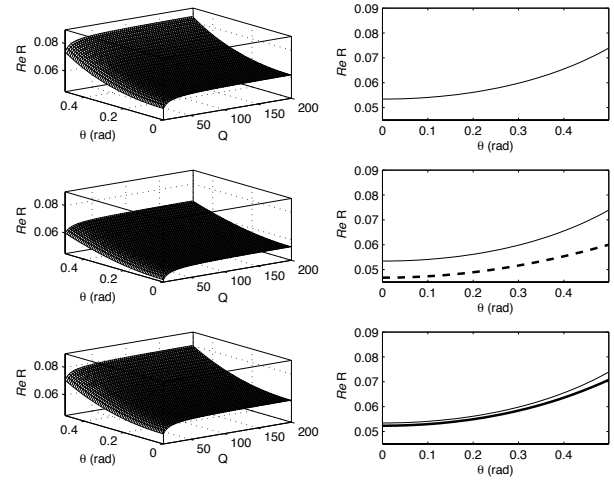

Figure 2: Absorptive reflection coefficient R, in exact and approximate forms, plotted over a range of oblique incidence angles and target Q values, with c_0 =1500m/s and c =1700m/s and a fixed mid-band ω. Left column, from top to bottom: surface plots of exact, linear, and nonlinear (second order) approximations. Right column: extractions from left column, for fixed target $Q = 10$, in which the exact R is represented with a solid line, the linear R with a dashed line, and the nonlinear (second order) R with a bold solid line.

where for any $\mathscr{Y}$, $\hat{\det}\mathscr{Y} \equiv \det\mathscr{Y}/\det\mathscr{A}^{(0)}$. Equations (8) and (9) are the anelastic extensions of equation (6), i.e., series formulas for the two reflection coefficients associated with a plane elastic P-wave incident upon an anelastic boundary. To evaluate the formulas we simply compute the necessary determinants and organize the results in orders of a_α, a_β, a_ρ, a_{Q_p} and a_{Q_s}. The formulas are a natural framework for approximation, but are themselves in principle exact, if the S_Y series and the series expansions of A, C and D are not truncated.

Let us illustrate by pursuing the simplest available example: for small contrasts we may approximate R_P and R_S linearly in any of the five perturbations, and accurate to order X^2, as:

$$\begin{aligned} R_P(\omega,\theta) &\approx \Gamma^P_\alpha a_\alpha + \Gamma^P_\beta a_\beta + \Gamma^P_\rho a_\rho + \Gamma^P_{Q_P} a_{Q_P} + \Gamma^P_{Q_S} a_{Q_S}, \\ R_S(\omega,\theta) &\approx \Gamma^S_\alpha a_\alpha + \Gamma^S_\beta a_\beta + \Gamma^S_\rho a_\rho + \Gamma^S_{Q_P} a_{Q_P} + \Gamma^S_{Q_S} a_{Q_S}, \end{aligned} \tag{10}$$

where

$$\begin{aligned} &\Gamma^P_\alpha = \frac{1}{4}(1+X^2),\ \Gamma^P_\beta = -2B^2X^2,\ \Gamma^P_\rho = \frac{1}{2}(1-4B^2X^2), \\ &\Gamma^P_{Q_P} = -\frac{1}{2}F_P(1+X^2),\ \Gamma^P_{Q_S} = 4F_SB^2X^2, \end{aligned} \tag{11}$$

and

$$\begin{aligned} &\Gamma^S_\alpha = 0,\ \Gamma^S_\beta = -BX,\ \Gamma^S_\rho = -\left(B+\frac{1}{2}\right)X, \\ &\Gamma^S_{Q_P} = 0,\ \Gamma^S_{Q_S} = 2BF_SX. \end{aligned} \tag{12}$$

In Figure 3, the coefficients R_P and R_S are plotted as functions of θ and $f = \omega/2\pi$ for parameters $\rho_0 = 2.1$g/cc, $\rho = 2.1$g/cc, $\alpha_0 = 3000$m/s, $\alpha = 3500$m/s, $\beta_0 = 1500$m/s, $\beta = 1700$m/s, $Q_P = 5$, and $Q_S = 5$. Exact coefficients are in the left column, linear approximations (i.e., $R_P \approx R_{P_1}$ and $R_S \approx R_{S_1}$) are in the center, and nonlinear approximations accurate two second order in the perturbations (i.e., $R_P \approx R_{P_1} + R_{P_2}$ and $R_S \approx R_{S_1} + R_{S_2}$) are in the right column. In all cases regimes of (small) angle are noted where the approximations are relatively accurate. In Figure 4, for instance, extractions of the same R_P and R_S are plotted vs. angle (left column) for fixed $f = 40$Hz, and vs. frequency (right column) for fixed $\theta = 11^\circ$.

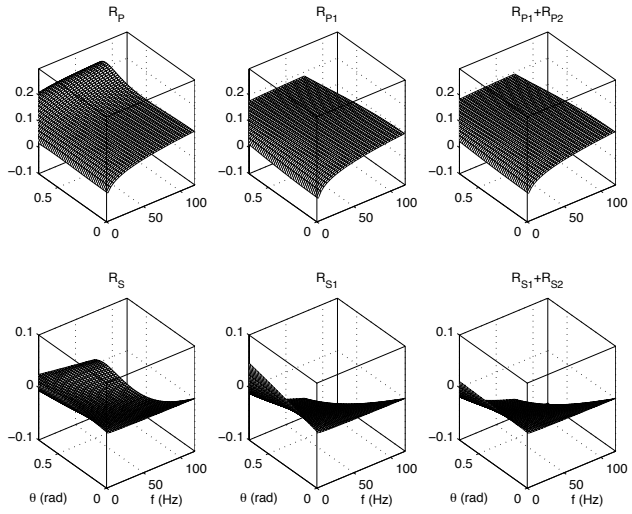

Figure 3: R_P and R_S plotted for a range of angles and frequencies. Left column: exact R_P and R_S, calculated using equation (2); middle column: R_P and R_S, accurate to first order in the perturbations and $\sin^2\theta$; right column: R_P and R_S accurate to second order in the perturbations and first order in $\sin^2\theta$.

INVERSION

We will begin to treat the AVF inverse problem by considering a wave field impinging at normal incidence on a plane contrast in c and Q. Setting $\theta = 0$ in equation (6), the requisite R has the form

$$R(\omega) = \left(\frac{1}{4}a_c - \frac{1}{2}F(\omega)a_Q\right) + \left(\frac{1}{8}a_c^2 + \frac{1}{4}F^2(\omega)a_Q^2\right) + \ldots \quad . \tag{13}$$

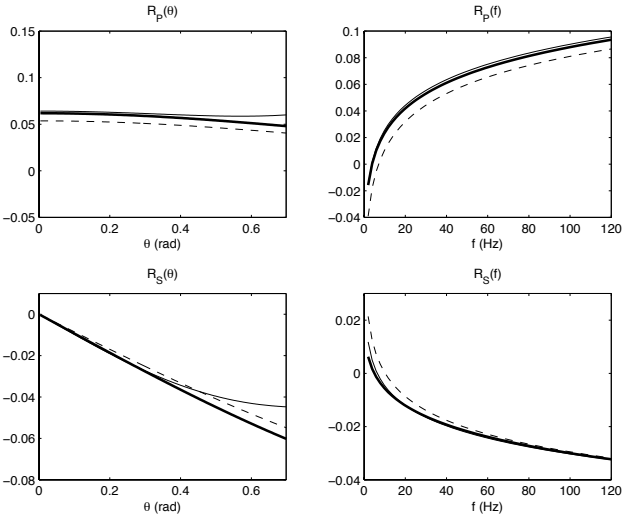

Figure 4: R_P and R_S values extracted from Figure 3. Left column: R_P and R_S plotted as functions of angle for fixed $f = \omega/2\pi = 40Hz$. Right column: R_P and R_S plotted as functions of frequency f for fixed $\theta = 11^\circ$. Exact coefficients are plotted as solid lines, first order approximations as dashed lines, and second order approximations as bold solid lines.

This expression is inverted by forming inverse series $a_c = a_{c_1} + a_{c_2} + \ldots$, and $a_Q = a_{Q_1} + a_{Q_2} + \ldots$, substituting them into equation (13), equating like orders, and summing the sequentially-determined components of a_c and a_Q. Using R at two angular frequencies, ω_1 and ω_2, we obtain, at first order,

$$\begin{aligned} a_{Q_1}(\omega_1,\omega_2) &= -2\left[\frac{R(\omega_1)-R(\omega_2)}{F(\omega_1)-F(\omega_2)}\right] \\ a_{c_1}(\omega_1,\omega_2) &= -4\left[\frac{F(\omega_2)R(\omega_1)-F(\omega_1)R(\omega_2)}{F(\omega_1)-F(\omega_2)}\right], \end{aligned} \tag{14}$$

and at second order

$$\begin{aligned} a_{Q_2}(\omega_1,\omega_2) &= \Delta_{Q_1}a_{Q_1} + \Delta_{Q_2}a_{c_1} \\ a_{c_2}(\omega_1,\omega_2) &= \Delta_{c_1}a_{Q_1} + \Delta_{c_2}a_{c_1}, \end{aligned} \tag{15}$$

where

$$\begin{aligned} &\Delta_{Q_1} = \frac{1}{2}[F(\omega_1)+F(\omega_2)], \Delta_{Q_2} = 0, \\ &\Delta_{c_1} = F_1F_2, \Delta_{c_2} = -\frac{1}{2}. \end{aligned} \tag{16}$$

In Figure 5 we illustrate the use of these formulas to invert for c and Q, using synthetically derived values of R at normal incidence for an acoustic medium (c_0 =1500m/s) overlying an absorptive medium (c =1800m/s, Q =10). Target medium properties are determined using R values at pairs of frequencies $f_1 = \omega_1/2\pi$, $f_2 = \omega_2/2\pi$ ranging from 2-120 Hz. In Figure 5, top left, the target Q value is recovered to first order for each frequency pair; bottom left, to second order. In Figure 5 top right, the target wavespeed value is recovered to first order; bottom right, to second order. In addition to the significant increase in accuracy from first to second order, we note that the spurious variation of the linear Q inversion result with experimental variables (in this case frequency), a characteristic of the inverse Born approximation, diminishes as order increases. Proximal frequencies, i.e., $f_1 \approx f_2$, evidently affect the conditioning of the second order recovery of c. Next we consider the anelastic problem. Taking differences of the R_P and R_S

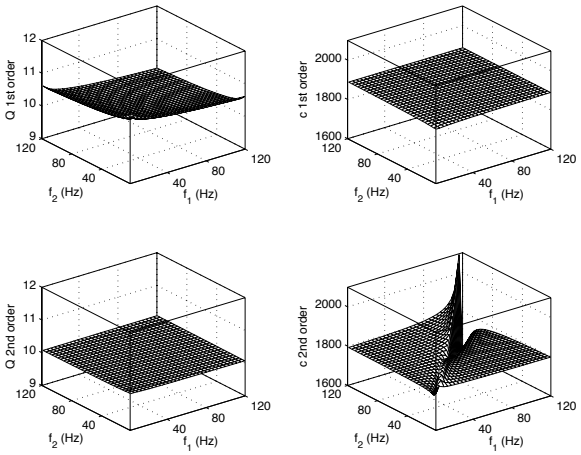

Figure 5: Target medium properties recovered over a range of frequency pairs, using exact synthetic R values, generated using equation (1) with $\theta = 0$, as input for the AVF inverse formulas in equations (14)–(15). Exact model values are $Q = 10$, $c = 1800$m/s. All c/Q values in rank deficient cases (i.e., where $f_1 = f_2$) are interpolated over.

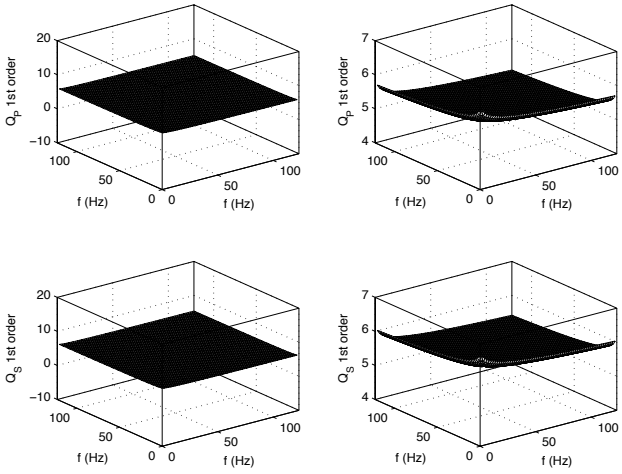

Figure 6: Recovered Q_P and Q_S values accurate to first order (actual values $Q_P = Q_S = 5$) using exact synthetic R_P, R_S values, calculated using equation (2), as input for the AVF inverse formulas in equations (17) and (19), over a range of frequency pairs and with $\theta = 11^\circ$. Left column: recovered Q_P, Q_S values; right column: detail of same.

coefficients for pairs of frequencies ω_1 and ω_2 permits the Q_P and Q_S perturbations to be solved for. The Q_S perturbation is solved for using R_S:

$$a_{Q_S} \approx \frac{R_S(\omega_1,\theta) - R_S(\omega_2,\theta)}{\Gamma^S_{Q_S}(\omega_1,\theta) - \Gamma^S_{Q_S}(\omega_2,\theta)}. \tag{17}$$

The Q_P perturbation may then be solved for through the difference

$$\begin{aligned} R_P(\omega_1,\theta) - R_P(\omega_2,\theta) = &\left[\Gamma^P_{Q_P}(\omega_1,\theta) - \Gamma^P_{Q_P}(\omega_2,\theta)\right] a_{Q_P} \\ &+ \left[\Gamma^P_{Q_S}(\omega_1,\theta) - \Gamma^P_{Q_S}(\omega_2,\theta)\right] a_{Q_S}, \end{aligned} \tag{18}$$

from which, and using equation (17),

$$\begin{aligned} a_{Q_P} \approx &\frac{R_P(\omega_1,\theta) - R_P(\omega_2,\theta)}{\Gamma^P_{Q_P}(\omega_1,\theta) - \Gamma^P_{Q_P}(\omega_2,\theta)} - \frac{\Gamma^P_{Q_S}(\omega_1,\theta) - \Gamma^P_{Q_S}(\omega_2,\theta)}{\Gamma^P_{Q_P}(\omega_1,\theta) - \Gamma^P_{Q_P}(\omega_2,\theta)} \\ &\times \left[R_S(\omega_1,\theta) - R_S(\omega_2,\theta)\right]. \end{aligned} \tag{19}$$

In Figure 6 we observe the results of applying these linearized formulas to synthetically derived reflection coefficients. Some care is required in choosing angles. For instance, our inverse formulas absent nonlinear correction rely on the $R_P \approx R_{P_1}$, $R_S \approx R_{S_1}$ approximations being accurate, hence θ should not be chosen too large. However, $R_S = 0$ at $\theta = 0$, hence if θ is chosen too small, the signal with which the shear parameter estimations are carried out will be too low (although, judging from equation (19), this may be an excellent regime in which to more straightforwardly estimate the compressive parameters). The angle used in Figure 4, $\theta = 11^\circ$, is also used here. In Figure 6, Q_P and Q_S are recovered for ranges of pairs of frequencies as before. Similar accuracies are noted in comparison to the two-parameter AVF results produced in equations (14)–(15).

This may proceed for the other parameters by varying θ, and for higher orders also, as we have illustrated in earlier sections. The key here is again to note that the core activity in the estimation of Q perturbations is the frequency differencing of the reflection coefficients. In spite of the increased complexity in terms of parameters and physical phenomena, we again discern that the basic data interrogation procedure seen in equation (14) is preserved.

DISCUSSION AND CONCLUSIONS

Application of absorptive AVF formulas of this type in the field will require the ability to extract an individual event from a seismic data set and estimate its local spectrum. Fortunately, a wide array of methods for determining and using these spectra to achieve seismic processing goals have been developed in recent years (e.g., Margrave, 1997; Margrave et al., 2003; Naghizadeh and Innanen, 2010). Although this introduces a new element to the problem not shared by elastic AVO methods, such tools are being more and more effectively created and used; in fact, the application of a time-frequency decomposition method led to the detection of one case of exactly the absorptive reflection coefficients we are considering (Odebeatu et al., 2006).

The nonlinear corrections would appear to be a key element of the inversion in the presence of low-Q targets. For instance, if the target Q value is in the range 5-10, the linearized estimate, depending on which data type and formula are used, could be in error by anywhere from 10-50%. In addition to reducing the bulk error, the second order correction "flattens" the estimate when it is plotted over all pairs of frequency or angle, meaning, the variation in accuracy of the results is lowered considerably. Nevertheless, the linearized estimates may often be more than sufficient to detect and roughly characterize the attenuative properties of a fluid target.

As with the more general problem of absorptive inverse scattering, the final aim is to cast the problem in a suitably complete anelastic environment, possibly coupled with anisotropy. Here we have lain the groundwork for development towards this end, but in doing so have demonstrated that certain properties of absorptive AVF (or, equivalently, AVA, although we have not explicitly demonstrated this here) inversion are independent of the complexity of the model type. In particular, differencing of reflection strengths across frequency evidently drives the procedure, whether in a two-parameter acoustic/absorptive physical setting or a five-parameter anelastic setting. We expect such generalities to remain as more complete versions of these methods are developed.

ACKNOWLEDGEMENTS

The sponsors of CREWES are gratefully acknowledged.